American Heart Association | American Stroke Association®

Associations Between Fibrocytes and Postcontrast Myocardial T$_1$ Times in Hypertrophic Cardiomyopathy

Lu Fang, PhD; Anna Beale, MBBS (hons), BMedSci (hons); Andris H. Ellims, MBBS; Xiao-lei Moore, PhD; Liang-han Ling, MBBS; Andrew J. Taylor, MBBS, PhD; Jaye Chin-Dusting, PhD; Anthony M. Dart, PhD, FRCP

Background—Fibrocytes are bone marrow-derived mesenchymal progenitors that have been linked to various fibrotic disorders. This study was undertaken to investigate whether fibrocytes are increased in diffuse myocardial fibrosis in humans.

Methods and Results—Thirty-seven patients with hypertrophic cardiomyopathy (HCM) and 20 healthy controls were recruited. Cardiac magnetic resonance imaging with postcontrast T$_1$ mapping was performed to non-invasively quantify diffuse myocardial fibrosis and these patients were classified into 2 groups (T$_1$<470 ms or T$_1$≥470 ms, as likely or unlikely to have diffuse fibrosis, respectively). Circulating fibrocytes (CD45+/CD34+/collagen I+) were measured by flow cytometry. Peripheral blood mononuclear cells (PBMCs) were cultured for 13 days and fibrocytes were quantitated by flow cytometry (CD45+/collagen I+) and real-time PCR (gene expression of matrix proteins). Plasma cytokines/chemokines mediating fibrocyte trafficking and differentiation were measured by multiplex assays. Circulating fibrocytes were decreased in HCM patients compared to controls. The proportion of fibrocytes derived from PBMCs was increased in patients with diffuse fibrosis compared with those without or controls (31.1±4.1% versus 18.9±3.9% and 10.9±2.0%, *P*<0.05 and *P*<0.001, respectively), and the proportion of fibrocytes was inversely correlated with T$_1$ time (*r*=−0.37, *P*=0.03). Plasma levels of stromal cell-derived factor-1 were elevated in patients with diffuse fibrosis compared with those without or controls (5131±271 pg/mL versus 3893±356 pg/mL and 4172±185 pg/mL, respectively, both *P*<0.05).

Conclusions—HCM patients with diffuse fibrosis as assessed by postcontrast T$_1$ mapping have elevated plasma SDF and an enhanced ability of PBMCs to differentiate into fibrocytes, suggesting that fibrocytes may contribute to the pathogenesis of myocardial fibrosis. (*J Am Heart Assoc.* 2013;2:e000270 doi: 10.1161/JAHA.113.000270)

Key Words: fibroblasts • hypertrophic cardiomyopathy • myocardial fibrosis • T$_1$ mapping

Myocardial fibrosis, a hallmark of various cardiovascular diseases, contributes to heart failure, and increased risk for arrhythmias and sudden death.[1,2] Hypertrophic cardiomyopathy (HCM) is a relatively common inherited cardiac disease defined by the presence of otherwise unexplained left ventricular hypertrophy associated with

non-dilated ventricular chambers.[3] Diffuse fibrosis (reactive fibrosis) and focal fibrosis (replacement fibrosis for necrotic myocytes) are common features of HCM,[4] contributing to the poor prognosis in these patients.[4,5] However, the pathogenesis of myocardial fibrosis is not completely understood.

The ability to identify myocardial fibrosis non-invasively has been transformed with the introduction of cardiac magnetic resonance (CMR) imaging.[6] Late gadolinium enhancement (LGE) is now an established method to identify focal myocardial fibrosis,[7,8] but it is unable to detect diffuse myocardial fibrosis.[4,7] Postcontrast myocardial longitudinal relaxation time (T$_1$) mapping is an emerging CMR technique that can evaluate diffuse myocardial fibrosis.[9] A number of T$_1$ mapping techniques have been shown to correlate with histologically quantified fibrosis.[9,10] Shortened T$_1$ times, consistent with the presence of diffuse myocardial fibrosis, have been reported in several cardiac disease states associated with diffuse fibrosis including heart failure,[9,11] ischemic heart disease,[12] diabetes,[13] and atrial fibrillation.[14] We recently found that postcontrast myocardial T$_1$ times were significantly lower in patients with

HCM compared with healthy controls and that lower postcontrast myocardial T$_1$ time was correlated with worsening diastolic dysfunction.[15.]

The primary source of collagen production in the heart has long been thought to be resident fibroblasts. However, cells from other sources such as endothelial-to-mesenchymal transition[16] and fibrocytes (bone marrow-derived mesenchymal progenitors)[17] may also contribute to myocardial fibrosis. Initial studies demonstrated that peripheral blood mononuclear cells (PBMCs) were capable of developing into fibrocytes after 10 to 14 days of culture.[17] Fibrocytes express a variety of mesenchymal markers, the leukocyte common antigen CD45, and the hematopoietic stem cell marker CD34. They produce matrix proteins and migrate to the sites of tissue injury where they become fibroblast-like cells.[18] A number of studies have found that fibrocytes not only participate in normal wound repair and tissue regeneration, but are also involved in aberrant wound healing and various fibrotic diseases.[19–24] Recent evidence has shown involvement of fibrocytes in mouse models with myocardial fibrosis,[25,26] however, fibrocytes have not been directly linked with myocardial fibrosis in humans.

Therefore, this project was designed to study: (1) whether increased numbers of circulating fibrocytes or increased differentiation potential of PBMCs into fibrocytes are found in HCM patients with diffuse myocardial fibrosis assessed by CMR; (2) whether fibrocyte number is associated with the extent of myocardial fibrosis, diastolic dysfunction, and circulating collagen turnover markers in those patients.

Methods

Study Subjects

Thirty-seven consecutive patients referred to the Alfred CMR department for the further evaluation of asymmetric septal hypertrophy (ASH) due to HCM from March 2011 to October 2012 were recruited. ASH was defined as an interventricular septum thickness of ≥15 mm with a ratio of septal-to-lateral wall thickness of ≥1.3:1.0 as measured by echocardiography, and the diagnosis of HCM required the absence of another condition that causes the degree of hypertrophy observed. Twenty asymptomatic subjects with no documented history of cardiovascular disease formed a healthy control group. Exclusion criteria included previous septal reduction therapy, coronary artery disease, atrial fibrillation, valvular heart disease, systemic hypertension, diabetes mellitus, surgery or trauma within previous 6 months, known fibrotic or inflammatory disease or cancer, contraindications to CMR, including pacemaker and defibrillator implantation, and significant renal dysfunction (estimated glomerular filtration rate [eGFR] <30 mL/min per 1.73 m^2). This study complied

with the Declaration of Helsinki and was approved by the Institutional Ethics Committee of Alfred Healthcare. Informed consent was obtained from all participants.

CMR

CMR was performed using a clinical 1.5-T scanner (Sigma HD 1.5-T, GE Healthcare). All sequences were acquired during a breath-hold of 10 to 15 seconds. Left ventricular (LV) volume and function were assessed by a contiguous short-axis steady-state free precession (SSFP) cine stack (repetition time [TR]=3.8 ms, echo time [TE]=1.6 ms, 30 phases) extending from the mitral valve annulus to the LV apex (slice thickness 8 mm, no gap).

Late gadolinium enhancement (LGE) imaging was performed using standard long-axis views of the LV and a contiguous short axis stack from the mitral valve annulus to the LV apex. LGE was evaluated 10 minutes after a bolus of gadolinium-diethylene triamine penta-acetic acid (DTPA) (0.2 mmol/kg BW Magnevist) to identify regional fibrosis using an inversion recovery gradient echo technique (TR 7.1 ms, TE 3.1 ms, inversion time [TI] individually determined to null the myocardial signal, range 180 to 250 ms, slice thickness 8 mm, matrix 256 × 192, number of acquisitions=2). Regional fibrosis was identified by LGE within the myocardium, defined quantitatively by a myocardial postcontrast signal intensity 6 SD above that within a reference region of remote myocardium (without LGE) within the same slice.

For the evaluation of diffuse myocardial fibrosis, a T$_1$ mapping sequence was used to cycle through acquisition of images obtained at the 3 standard short-axis levels (basal, mid, and apical) over a range of inversion times. The sequence consisted of an electrocardiogram-triggered, inversion-recovery prepared, two-dimensional fast gradient echo sequence employing variable temporal sampling of k-space (VAST) (Global Applied Science Laboratory, GE Healthcare). Ten images were acquired sequentially at increasing inversion times (75 to 750 ms), commencing 20 minutes after the bolus of gadolinium–DTPA and over a series of 3 to 5 breath-holds. Imaging parameters were TR/TE: 3.7/1.2 ms, flip angle: 20°, 256×128 acquisition matrix, 36×27 cm field of view, slice thickness 8 mm, TI: 75 to 750 ms, trigger delay 300 ms, and views per segment=24. These images were then processed with a curve fitting technique to generate T$_1$ maps. Following image acquisition, the ten short-axis images of varying inversion times were transferred to an external computer for analysis using a dedicated research software package (Cinetool, Global Applied Science Laboratory, GE Healthcare). This provided the ability to analyze regions of interest (ROIs) to find average T$_1$ for that area, as well as a pixel-by-pixel determination of T$_1$, by fitting data acquired at various preparation times to the exponential curve:

M_z (t=TI)=M_0(A−B[$e^{-t/T1}$=]), relating the sample magnetization M_z observed at the time t=TI to the equilibrium magnetization M_0 and sample T_1, where TI denotes inversion time for an inversion recovery experiment. For each short-axis image, an ROI was drawn around the entire LV myocardium (excluding papillary muscles) to calculate postcontrast myocardial T_1 time. In subjects with regional fibrosis detected by LGE, these areas were excluded from the ROI for the primary analysis of postcontrast myocardial T_1 time. T_1 times for ROIs including areas of LGE were also calculated. To account for the potential effects of glomerular filtration rate, time delay postcontrast administration, and contrast agent relaxivity on gadolinium pharmacokinetics, corrected values of T_1 times were used to normalize postcontrast myocardial T_1 times to a matched state (time postcontrast administration=20 minutes, eGFR=90 mL/min per 1.73 m^2).[27] In addition, raw postcontrast T_1 times of the LV blood pool (blood T_1 times) were calculated.

Echocardiography

Transthoracic echocardiography with a standard clinical protocol was performed immediately prior to CMR. Diastolic function was assessed by a combination of mitral inflow pattern (E to A ratio and deceleration time) and mitral annular velocities (e', measured at the septal and lateral aspects of the mitral annulus in the apical 4-chamber view). Additionally, mitral E/e' (septal, lateral, and mean) was chosen as an index of LV filling pressure. Echocardiography was performed in 27 HCM patients and 18 controls.

Blood Sample Collection

Blood samples were collected into EDTA-tubes by venepuncture. Two to 3 mL blood was sent to Alfred Pathology Department for full blood count measurement. A further 2 mL of whole blood was allocated for measuring circulating fibrocytes by flow cytometry (see below). Plasma samples were stored at −80°C for cytokine and chemokine measurement (detailed below). The remaining blood (after removal of plasma) was diluted with phosphate-buffered saline (PBS) and used for PBMC isolation as per below. Serum was collected from an additional tube without anticoagulants for measurement of amino terminal propeptide of type I and III collagen (PINP and PIIINP) by radioimmunoassay at Alfred Pathology Department.

Measurement of Circulating Fibrocytes

Circulating fibrocytes were measured by flow cytometry as was previously described.[28] An amount of 200 μL of whole blood was aliquoted to each FACS tube. After red blood cells were lysed with lysing buffer (BD Bioscience), white blood cells (WBC) were incubated with anti-collagen I antibody (5 μL, Millipore) for 30 minutes on ice, and washed twice with PBS containing 1% fetal bovine serum (FBS), followed by incubation with fluorescein isothiocyanate (FITC)-conjugated secondary anti-mouse antibody (1 μL, Millipore) for 30 minutes on ice and washed twice. Cells were then further stained with allophycocyanin (APC)-conjugated anti-CD45 antibody (10 μL) and phycoerythrin (PE)-conjugated anti-CD34 antibody (7.5 μL) or respective isotype control antibodies (BD Bioscience) for 30 minutes on ice and washed twice. WBC (≈500 000/sample) were acquired with a Becton-Dickinson FACSCalibur and data analyzed with FlowJo software (Tree Star). Compensation was calculated with CompBeads (BD Bioscience) stained with single-color antibody (FITC, PE, and APC). CD45$^+$ cells were gated using isotype control and cells gated for CD45 were further analyzed for collagen I and CD34 expression against isotype controls.

Measurement of Fibrocytes From PBMC Culture

The method of culturing fibrocytes from PBMCs was described previously.[28,29] PBMCs were isolated with the use of a Ficoll-Paque plus (Amersham Biosciences) according to the manufacturer's instruction. As described above, remaining blood was diluted with PBS (1:2) and layered on top of Ficoll-Paque and centrifuged at 400g for 30 minutes at room temperature. The mononuclear cell layer was carefully collected and rinsed twice with PBS. PBMCs were suspended in DMEM supplemented with 10% fetal bovine serum, 2 mmol/L L-glutamine and 1% antibiotics-antimycotics, and plated at a density of 2×10^6 cells/mL in fibronectin-coated 6-well plates (2.5 mL/well) and incubated at 37°C with 5% CO_2. After 3 days, non-adherent cells were removed and adherent cells were further cultivated until 13 days. Media were refreshed every 3 days. Cells were then detached with accutase (Sigma) and aliquoted to 3×10^4 cells per FACS tube in 100 μL PBS and then measured by flow cytometry using 2 markers CD45 and collagen I (because cultured cells gradually lost CD34 expression) as described above. Approximately 2×10^4 events were acquired for each sample.

Gene Expression of Matrix Proteins and Chemokine Receptors

Total RNA was isolated from adherent cells with Trizol Reagent$^\circledR$ (Invitrogen) after 13 days' culture and reverse transcribed into cDNA using random primers and M-MLV reverse transcriptase (Invitrogen). Real-time PCR was performed using SYBR green kit (Roche) on an ABI Prism 7500 system (Applied Biosystems). The transcript abundance was expressed as fold increase over the value of healthy controls calculated by $2^{-\Delta\Delta Ct}$ method. The expression of targeted

genes (collagen I, vimentin, fibronectin, CXCR4, and CCR7) was normalized to 18s. Primer sequences are provided in Supplementary material online, Table S1.

Plasma Levels of Cytokines and Chemokines

Plasma levels of cytokines/chemokines promoting differentiation (transforming growth factor-β [TGF-β], interleukin [IL]-4 and -13),[30] inhibiting differentiation (interferon-γ [IFN-γ], IL-12, and serum amyloid P [SAP]),[30] and promoting trafficking (stromal cell-derived factor [SDF]-1 and secondary lymphoid-tissue chemokine [SLC] through interacting with CXCR4 and CCR7, respectively[24,31] as well as monocyte chemotactic protein [MCP]-1) of fibrocytes were measured using multiplex kits from Millipore according to the manufacturer's instruction, as we previously described.[28] The appropriate cytokine/chemokine standards, plasma samples (25 μL), and fluorescent conjugated, antibody-immobilized beads were added to wells of a pre-wet filtered plate and then were incubated overnight at 4°C. The following day, the plate was washed twice with wash buffer and then incubated with secondary detection antibody for 1 hour, followed by subsequent incubation with strepavidin-PE for 30 minutes. After the plate was washed twice again with wash buffer, it was read on the Luminex system (Biorad) with the addition of sheath fluid. Concentrations of different analytes in the plasma samples were determined by using respective standard curves generated in the multiplex assays. Neat plasma samples were used for all assays except for SAP and TGF-β1 (1:2000 and 1:30 dilution, respectively, using assay buffer provided in the kits).

Statistics

Data were expressed as mean±SD unless otherwise stated. SPSS 17.0 was used for statistical analysis. The normality of data was tested by Kolmogorov-Smirnov test. To compare differences among 3 groups, 1-way ANOVA followed by Tukey multiple comparison tests or Kruskal-Wallis H tests were used for parametic or nonparametric data, respectively. Pearson's correlation was used to assess correlations between parameters. Chi-square test was used to compare discrete variables among groups. A difference of $P<0.05$ (2-sided) was considered statistically significant.

Results

Patient Demographics

Patient demographics are presented in Table 1. The normal range of postcontrast myocardial T$_1$ times in healthy controls in our previous study was 561±47 ms,[15] so T$_1$ time (excluding

regions of LGE) of 470 ms (about 2 SD below the mean of control values) was chosen to divide the HCM cohort into those likely to have diffuse myocardial fibrosis (<470 ms) and those unlikely to have diffuse myocardial fibrosis (≥470 ms). Body mass index was significantly increased in HCM patient compared with controls. There were no significant differences in age, height, eGFR, heart rate, and blood pressure among the 3 groups. There were no differences in family history and medication (except angiotensin receptor blockers) between the 2 subgroups of HCM patients. WBC, neutrophils, and monocytes were significantly elevated in HCM patients compared to controls, but the percentage of monocytes was comparable among the 3 groups.

CMR and Echocardiograph Findings

CMR and echocardiograph findings are shown in Table 2. Postcontrast myocardial T$_1$ times excluding LGE were 568.5±49.2, 540.9±68.1, and 434.8±28.9 ms for control group, T$_1$≥470 ms group and T$_1$<470 ms group, respectively. When regions of LGE were included in the analysis of HCM patients, a further reduction in original values of T$_1$ times were observed (529.2±76.7 and 427.2±30.6 ms for the 2 subgroups, respectively). After correction for GFR and time delay postcontrast administration, T$_1$ times were 550±47.5, 519.2±75.4, and 417.2±32.9 ms for control group, T$_1$≥470 ms group, and T$_1$<470 ms group, respectively. There was no significant difference in raw blood T$_1$ times among the 3 groups, effectively ruling out contrast kinetics as a confounding factor for the observed differences in myocardial T$_1$ time between groups. As expected, septal wall thickness and the ratio of septal-to-lateral wall thickness were greater in both HCM groups compared with controls. The LV mass indexed to body surface area (BSA) was significantly increased in HCM patients compared with controls. Both HCM groups had normal systolic function. LGE (focal fibrosis) was observed in the majority of HCM patients (absent in 2 patients with diffuse fibrosis and 3 patients without diffuse fibrosis) and the mean quantity of LGE was comparable between the 2 HCM groups. Left atrial volume indexed to BSA and resting left ventricular outflow tract gradient were significantly higher while septal, lateral, and mean e' were significantly lower in HCM patients compared to controls. Deceleration time and septal, lateral, and mean E/e' were significantly higher in patients with diffuse fibrosis compared to controls. Mean E/e' was inversely correlated with T$_1$ time ($r=-0.57$, $P<0.001$, Figure 1A).

Circulating Markers of Collagen Turnover

PINP and PIIINP are markers reflecting the status of collagen turnover. Neither PINP nor PIIINP significantly differed among the 3 groups (Figure 1B).

Table 1. Subject Characteristics

	Control	T$_1$≥470	T$_1$<470
n	20	21	16
Gender, m/f	14/6	13/8	14/2
Age, y	46±13	49.6±14.6	48.7±13.8
Height, cm	175.2±11.3	167.2±11.2	174.8±9.1
Weight, kg	70.8±11.3	75.5±20.2	85.8±15.2*
Body mass index, kg/m^2	22.6±2.2	26.6±4.7**	28±4.0***
Family history of HCM, %	NA	31.6	18.8
Resting heart beat, beats/min	62.8±8.7	62.1±12.1	60.5±9.3
Systolic blood pressure, mm Hg	120.4±10.2	131.5±16.5	127±9.8
Diastolic blood pressure, mm Hg	73±9.8	73.4±9	73.6±9.9
eGFR, mL/min per 1.75 m^2	86.4±4.5	85.7±8.3	91±1
Medications			
β-blockers, %	NA	52.4	56.3
Calcium channel blockers, %	NA	14.3	31.3
Angiotensin convert enzyme inhibitor, %	NA	9.5	0
Angiotensin receptor blockers, %	NA	23.8	0[†]
Full Blood Count			
Haemoglobin, g/L	144.7±9.7	144.1±11.4	149.1±17.6
Platelets, 10^9/L	219.2±42.5	207.2±53.6	212.5±62.1
Hematocrit, L/L	0.42±0.03	0.42±0.03	0.43±0.05
White blood cells, 10^9/L	5.78±1.23	7.27±2.50*	8.39±1.97**
Neutrophils, 10^9/L	3.26±1.04	4.75±2.18*	5.53±1.90**
Lymphocytes, 10^9/L	1.91±0.56	1.87±0.61	2±0.55
Monocytes, 10^9/L	0.39±0.12	0.51±0.17*	0.53±0.16*
Monocytes, % of WBC	6.84±1.84	7.28±1.89	6.48±1.50

Data are expressed as mean±SD. eGFR indicates estimated glomerular filtration rate; HCM, hypertrophic cardiomyopathy; WBC, white blood cells.
*P<0.05, **P<0.01, ***P<0.001, vs controls, [†]P<0.05 vs T$_1$≥470 ms.

Circulating Fibrocytes

We measured the percentage of circulating fibrocytes expressed relative to the whole population of WBC (CD45+) in fresh blood by flow cytometry using 3 markers (CD45/CD34/collagen I) (Figure 2A). The percentage of circulating fibrocytes was then multiplied by WBC count to determine the concentrations of fibrocytes per microliter of blood. HCM patients had a significant lower percentage of circulating fibrocytes compared to controls (0.07±0.01% versus 0.12±0.02%, P<0.05). The difference in the percentage of circulating fibrocytes between HCM patients without diffuse fibrosis and controls was also statistically significant (Figure 2B, P<0.05), but the change in the concentration of circulating fibrocytes per microliter of blood was not significant among the 3 groups (Figure 2B).

Fibrocytes Differentiated From PBMC Culture

A proportion of PBMCs differentiated into fibrocytes, which appear as spindle-shaped cells (Figure 3A) after 13 days' culture. Because cultured cells gradually lose CD34 expression, 2 markers (CD45/collagen I) were used to identify fibrocytes (Figure 3B). The proportion of fibrocytes derived from PBMCs was significantly increased in patients with diffuse fibrosis compared to those without diffuse fibrosis or controls (Figure 3C). Furthermore, the proportion of fibrocytes was inversely correlated with postcontrast myocardial T$_1$ time (r=−0.37, P=0.03, Figure 3D), but did not correlate with either the prevalence or the mean quantity of LGE. Fibrocytes from culture were also inversely correlated with septal, lateral, and mean e' (r=−0.46, P=0.007; r=−0.38, P=0.024; and r=−0.43 P=0.009, respectively), and positively correlated with deceleration time (r=0.48, P=0.003).

Table 2. CMR and Echocardiography Data

CMR Data	Control (20)	$T_1 \geq 470$ (21)	$T_1 < 470$ (16)
T_1 times (ms), excluding LGE	568.5±49.2	540.9±68.1	434.8±28.9***, ††
T_1 times (ms), including LGE	568.5±49.2	529.2±76.7	427.2±30.6***, ††
T_1 times (ms, corrected values)	550±47.5	519.2±75.4	417.2±32.9***, ††
Blood T_1 times, ms	306±21.5	308.1±32.5	299.9±24.2
Septal thickness, mm	8.3±1.6	18.9±6.2***	18.7±3.6***
Lateral wall thickness, mm	7.8±1.2	8.4±1.9	8.5±2.1
Septal/lateral wall thickness	1.06±0.09	2.29±0.54***	2.29±0.49***
LV mass index, g/BSA	51.4±8.9	86.6±37.8**	104.4±31.5***
LV ejection fraction, %	64.2±4.6	68.1±6.2	70±8.6
Presence of LGE, %	NA	85.7	87.5
Quantity of LGE (% of LV) mass	NA	5.6±7.8	5.3±6.7
Echocardiography data	Control (18)	$T_1 \geq 470$ (13)	$T_1 < 470$ (14)
Left atrial volume indexed, mL/m^2	27.6±8.9	40.8±9.0**	46.8±16.9***
E/A ratio	1.38±0.36	1.11±0.35	1.41±0.39†
Deceleration time, ms	182.1±27.0	188±45.7	232.5±47.1*
Septal e', cm/s	10.6±2.9	6.3±1.6***	6.1±1.9***
Lateral e', cm/s	13.7±3.5	8.8±2.8**	8.2±3.5***
Mean e', cm/s	11.9±3.0	7.5±1.9***	7±2.5***
Septal E/e'	8.5±2.6	11.9±3.9	14.3±5.6**
Lateral E/e'	6.3±1.9	8.7±2.8	11.8±6.1**
Mean E/e'	7.8±2.6	10.6±3.0	13.1±5.3**
Resting LVOT gradient, mm Hg	5.2±1.2	32±43.8*	36.2±45.9*

Data are expressed as mean±SD. BSA indicates body surface area; CMR, cardiac magnetic resonance; LGE: late gadolinium enhancement; LV, left ventricular; E/A, the ratio of the early (E) to late (A) ventricular filling velocities; E/e', the ratio of the early mitral filling velocity (E) to early diastolic mitral annular velocity (e'); LVOT, left ventricular outflow tract; T_1 times (corrected values), T_1 times were normalized to a matched state (time postcontrast administration=20 minutes, eGFR=90 mL/min per 1.73 m^2) to account for the potential effects of glomerular filtration rate, time delay postcontrast administration, and contrast agent relaxivity on gadolinium pharmacokinetics.

*$P<0.05$, **$P<0.01$, ***$P<0.001$, vs controls, †$P<0.05$, ††$P<0.001$, vs $T_1 \geq 470$ ms.

Gene Expression of Matrix Proteins and Chemokine Receptors on Cultured Cells

Expression of collagen and vimentin on the remaining adherent cells in the culture plate after 13 days' culture was upregulated in patients with diffuse fibrosis compared with controls ($P<0.05$, Figure 4A and 4B). Fibronectin expression was also upregulated in patients with diffuse fibrosis compared to those without diffuse fibrosis or controls ($P<0.05$, Figure 4C). There was no significant difference among groups for expression of the chemokine receptor CXCR4 (Figure 4D). Notably, CCR7 was very weakly expressed in these cells (data not shown).

Plasma Cytokines and Chemokines Mediating Fibrocyte Trafficking and Differentiation

Plasma SDF-1 was significantly elevated in HCM patients with diffuse fibrosis compared with those without diffuse fibrosis

or controls ($P<0.05$, Figure 5A), and was inversely correlated with postcontrast myocardial T_1 time ($r=-0.33$, $P=0.03$). There were no significant differences among groups for plasma levels of SLC, MCP-1, IFN-γ, IL-12, SAP, IL-4, IL-13, and TGF-β (Figure 5A and 5B).

Discussion

Myocardial fibrosis is a hallmark of cardiovascular disease; however its pathophysiology has not been fully understood. Fibrocytes have been linked to various fibrotic disorders,[19–21] but they have not been explored in patients with myocardial fibrosis. The main aim of this study was to investigate whether fibrocytes were increased in HCM patients with diffuse myocardial fibrosis. CMR postcontrast myocardial T_1 time, an emerging technique to detect and quantify diffuse myocardial fibrosis, was used to separate HCM patients into 2 subgroups ($T_1 < 470$ ms or $T_1 \geq 470$ ms as likely or unlikely
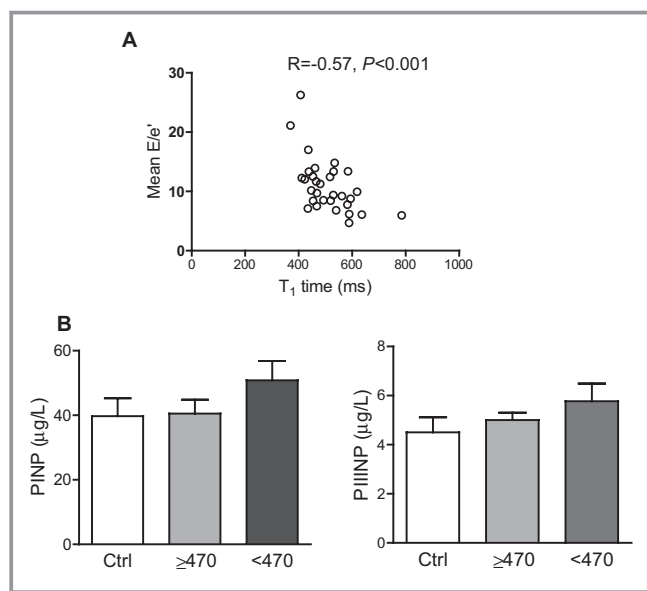
Figure 1. Correlation between postcontrast myocardial T$_1$ times and mean E/e' and circulating markers of collagen turnover. A, T$_1$ time (measured by CMR) was inversely correlated with mean E/e' (measured by echocardiograph), $r=-0.57$, $P<0.001$. B, Circulating markers of collagen turnover. Data were expressed as mean±SEM. CMR indicates cardiac magnetic resonance; PINP, aminoterminal propeptide of type I collagen, PIIINP, amino terminal propeptide of type III collagen; SEM, standard error of the mean.

to have diffuse myocardial fibrosis, respectively). We found that postcontrast myocardial T$_1$ time was inversely correlated with E/e', an index for diastolic dysfunction. Patients with diffuse fibrosis had a significantly higher yield of fibrocytes from PBMC culture, as indicated by a higher percentage of CD45+/collagen I+ fibrocytes and upregulated gene expression of matrix proteins, as compared to those without diffuse fibrosis or controls. Furthermore, fibrocytes derived from PBMCs were inversely correlated with postcontrast myocardial T$_1$ time and septal, lateral, and mean e', indicating a link between cultured fibrocytes and the extent of diffuse fibrosis and diastolic dysfunction. In addition, plasma SDF was elevated in HCM patients with diffuse fibrosis. However, HCM patients had a lower percentage of circulating fibrocytes compared to controls. Circulating PINP and PIIINP did not increase in patients with diffuse fibrosis. Taken together, patients with diffuse myocardial fibrosis as assessed by postcontrast myocardial T$_1$ time show elevated plasma SDF and an enhanced ability of PBMCs to differentiate into fibrocytes, suggesting that increased fibrocyte trafficking and differentiation may contribute to the pathogenesis of diffuse myocardial fibrosis in HCM.

Previous clinical studies have shown increased fibrocytes in patients with burns, asthma, systemic sclerosis, and idiopathic pulmonary fibrosis.[23,32–34] Two recent papers also reported accumulation of fibrocytes in mouse models of
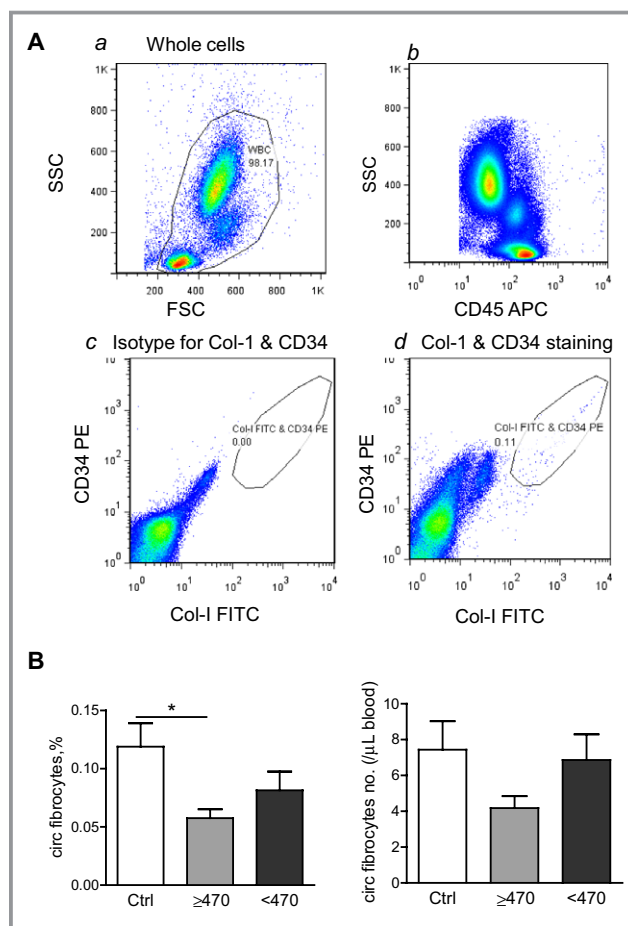
Figure 2. Measurement of circulating fibrocytes. A, Representative flow cytometric analysis of circulating fibrocytes. (a) Total cells acquired; (b) CD45+ cells; (c) Isotype control for collagen I and CD34 set on CD45+ cells; (d) Positive staining for collagen I and CD34 set on CD45+ cells; B, Circulating fibrocytes in patients with postcontrast myocardial T$_1$<470 ms (n=16), patients with T$_1$≥470 ms (n=21), and healthy controls (Ctrl, n=20). (a) The percentage of fibrocytes relative to white blood cells (WBC, i.e. CD45+); (b) the concentration of fibrocytes per microliter of blood. Data were expressed as mean±SEM (standard error of the mean). *$P<0.05$. APC indicates allophycocyanin; FITC, fluorescein isothiocyanate; FSC, forward scatter; PE, phycoerythrin; SSC, side scatter.
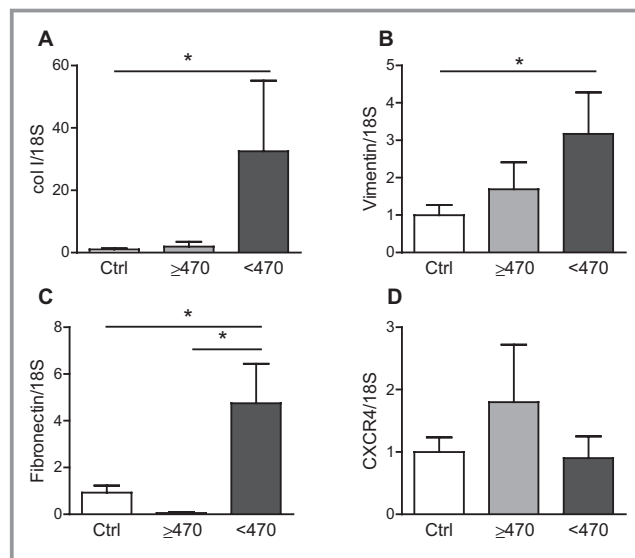
myocardial fibrosis.[25,26] Chu et al found that mice with chronic heart failure had greater collagen staining of their myocardium compared to controls, and that 20% of collagen I+ cells were fibrocytes.[25] Sopel et al also found increased CD133+/α-SMA+ fibrocytes in myocardial sections of mice with angiotensin II-induced myocardial fibrosis.[26] Our study is the first to associate fibrocytes with myocardial fibrosis in humans. After culturing adherent PBMCs for 13 days, we found significantly increased CD45+/collagen I+ fibrocytes in patients with diffuse fibrosis. This was supported by an increase in gene expression of matrix proteins (collagen I, vimentin, and fibronectin) of cultured cells, as it is well established that fibrocytes express matrix proteins.[17,35]
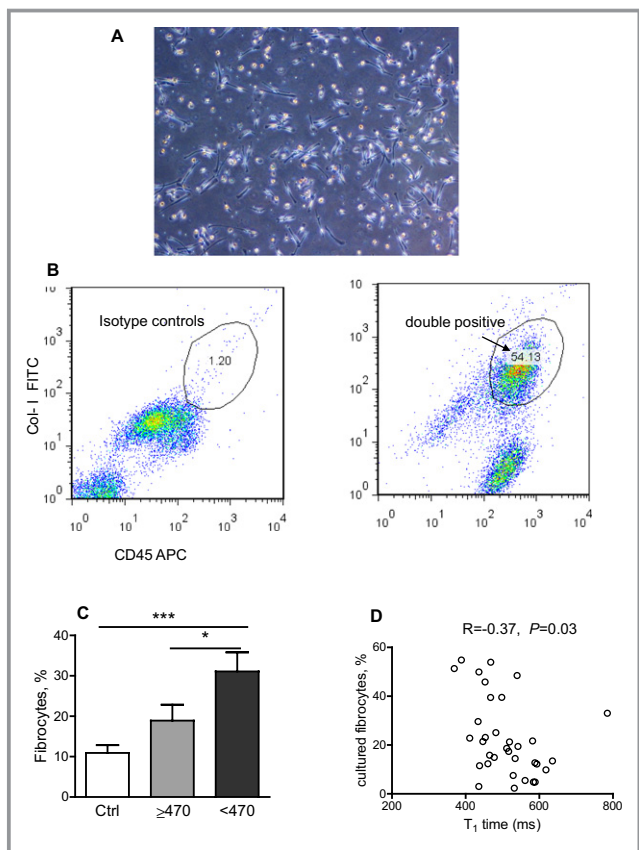
Figure 3. Differentiation of fibrocytes from PBMCs. A, Pictures of fibrocytes appeared as spindle-shaped cells developed from PBMC culture for 13 days (under ×40). B, Representative of flow cytometric dotplots of cells stained with CD45 and collagen I (left: isotype control, right: antibody staining) and double-positive cells are fibrocytes. C, The percentage of fibrocytes from PBMC culture relative to the remaining adherent cells in HCM patients with postcontrast myocardial T$_1$ time <470 ms, with T$_1$ time ≥470 ms and healthy controls (Ctrl) (n=16, 21, and 20, respectively). D, Correlation between cultured fibrocytes and T$_1$ time. Data were expressed as mean±SEM. *P<0.05; ***P<0.001. HCM indicates hypertrophic cardiomyopathy; PBMCs, peripheral blood mononuclear cells; SEM, standard error of the mean.


Figure 4. Gene expression of matrix proteins and chemokine receptors. Gene expression of collagen I (A), vimentin (B) and fibronectin (C), and CXCR4 (D) of the remaining adherent cells after PBMC culture for 13 days was measured by real-time PCR in HCM patients with postcontrast myocardial T$_1$ time <470 ms, with T$_1$ time ≥470 ms and healthy controls (Ctrl) (n=11, 6, and 14, respectively). Data were expressed as mean±SEM. *P<0.05. HCM indicates hypertrophic cardiomyopathy; PBMC, peripheral blood mononuclear cell; PCR, polymerase chain reaction; SEM, standard error of the mean.

Furthermore, the proportion of fibrocytes differentiated from PBMCs was inversely correlated with postcontrast myocardial T$_1$ time, but not with LGE.

In contrast to fibrocytes derived from PBMCs, the fibrocyte number in the peripheral blood was not increased in patients with diffuse fibrosis, which may be due to increased migration of circulating fibrocytes into the myocardium in these patients. SDF-1/CXCR4 axis plays a particularly important role in fibrocyte migration.[31,36] In this study, plasma SDF-1 was elevated in patients with diffuse fibrosis and inversely correlated with postcontrast myocardial T$_1$ time. This suggests that trafficking of fibrocytes from circulation into the myocardium could be increased in HCM patients with diffuse fibrosis. Chu et al[25] also reported elevated plasma SDF-1 in

patients with heart failure, and a diffuse increase in the expression of myocardial SDF-1 in mice with heart failure. They further demonstrated that cardiomyocytes secreted SDF-1.[25] Thus, increased plasma SDF-1, likely resulting from stimulated myocardium, promotes fibrocytes to infiltrate into the myocardium, subsequently contributing to myocardial fibrosis. Previous studies showed that blockade of SDF reduced infiltrating fibrocytes in mouse models of lung fibrosis.[31] Further studies are needed to investigate whether blockade of SDF could also attenuate myocardial fibrosis in experimental models through inhibiting recruitment of fibrocytes into the myocardium.

A previous study[37] reported that some healthy individuals had lower numbers of fibrocytes produced by PBMCs compared with others, and that adding conditioned medium from PBMC with high yield of fibrocytes into PBMCs with low yield of fibrocytes did not increase the fibrocyte number, indicating that the low yield of fibrocytes developed from PBMCs in some individuals may be due to intrinsic properties of their monocytes. In the present study, we did not observe significant differences in chemokines/cytokines mediating fibrocyte differentiation, which suggests that increased fibrocytes after PBMC culture may be due to an intrinsic predisposition of monocytes to differentiate into fibrocytes. These monocytes may be "preprogrammed" to adopt the
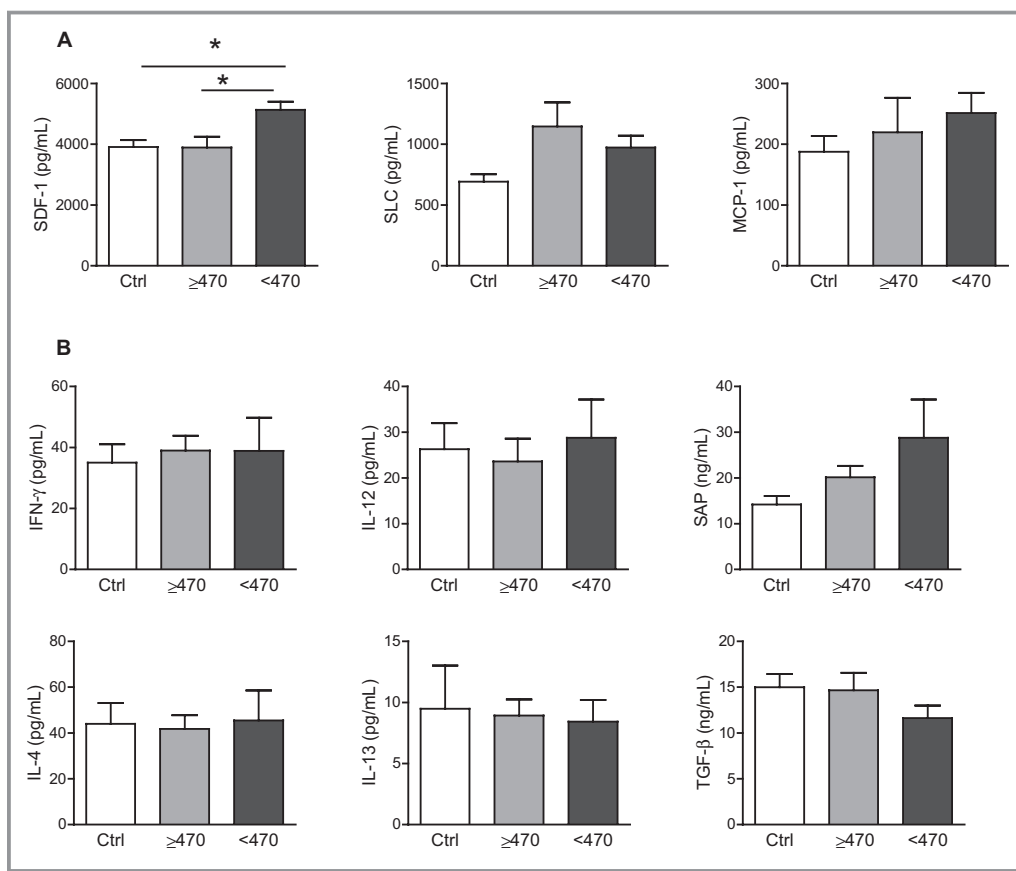
Figure 5. Changes of plasma chemokines/cytokines. Plasma levels of cytokines and chemokines mediating fibrocyte trafficking (A) and differentiation (B) were measured by multiplex assay in HCM patients with postcontrast myocardial T$_1$ time <470 ms, with T$_1$ time ≥470 ms and healthy controls (Ctrl) (n=16, 21, and 20, respectively). Data were expressed as mean±SEM. *P<0.05. HCM indicates hypertrophic cardiomyopathy; IFNγ, interferon γ; IL-4, interleukin-4; IL-12, interleukin-12; IL-13, interleukin-13; MCP-1, monocyte chemoattractant protein-1; SAP, serum amyloid P; SDF-1, stromal-derived factor-1; SLC, secondary lymphoid cytokine; TGFβ, transforming growth factor β; SEM, standard error of the mean.

fibrocyte phenotype, perhaps through genetic or epigenetic changes in progenitor cells, rather than relying purely on external influences.

Gai et al[27] proposed a method to normalize postcontrast myocardial T$_1$ times for GFR and time delay postcontrast administration to allow for comparison of T$_1$ times between different patients. In this study, we also calculated corrected T$_1$ times for all the subjects (Table 2) according to their method. The findings of the study are similar whether we use directly measured T$_1$ times or corrected T$_1$ times. We find a similar inverse correlation between corrected T$_1$ times and the proportion of fibrocytes derived from PBMC culture (r=−0.39, P=0.02). We used directly measured T$_1$ times throughout the text because correction of T$_1$ times is a relatively newly proposed method that may require further validation before being used as the only form in which T$_1$ data is presented.

The present study has several limitations. First, postcontrast myocardial T$_1$ times are also affected by other factors that may expand the extracellular matrix, so T$_1$ times are not specific for diffuse myocardial fibrosis. Second, the

sample size of the present study is relatively small, so we did not adjust for multiple factors when we assessed the association between fibrocytes and T$_1$ times. Some of the tests may also have failed to reach statistical significance due to low power. Therefore, larger sample sizes would be needed for future studies.

In conclusion, HCM patients with diffuse fibrosis as assessed by postcontrast myocardial T$_1$ time have elevated plasma SDF and an enhanced ability of PBMCs to differentiate into fibrocytes, suggesting that fibrocytes may contribute to the pathogenesis of diffuse myocardial fibrosis in HCM. Future studies need to be conducted to investigate whether inhibition of fibrocyte trafficking or differentiation attenuates diffuse myocardial fibrosis.

Sources of Funding

Disclosures

None.

References

1. Dobaczewski M, Frangogiannis NG. Chemokines and cardiac fibrosis. *Front Biosci (Schol Ed)*. 2009;1:391–405.

2. Zile MR, Brutsaert DL. New concepts in diastolic dysfunction and diastolic heart failure: Part II: causal mechanisms and treatment. *Circulation*. 2002;105:1503–1508.

3. Maron BJ. Hypertrophic cardiomyopathy: a systematic review. *JAMA*. 2002; 287:1308–1320.

4. Varnava AM, Elliott PM, Sharma S, McKenna WJ, Davies MJ. Hypertrophic cardiomyopathy: the interrelation of disarray, fibrosis, and small vessel disease. *Heart*. 2000;84:476–482.

5. Shirani J, Pick R, Roberts WC, Maron BJ. Morphology and significance of the left ventricular collagen network in young patients with hypertrophic cardiomyopathy and sudden cardiac death. *J Am Coll Cardiol*. 2000;35:36–44.

6. Mewton N, Liu CY, Croisille P, Bluemke D, Lima JA. Assessment of myocardial fibrosis with cardiovascular magnetic resonance. *J Am Coll Cardiol*. 2011;57: 891–903.

7. Kim RJ, Judd RM. Gadolinium-enhanced magnetic resonance imaging in hypertrophic cardiomyopathy: in vivo imaging of the pathologic substrate for premature cardiac death? *J Am Coll Cardiol*. 2003;41:1568–1572.

8. Teraoka K, Hirano M, Ookubo H, Sasaki K, Katsuyama H, Amino M, Abe Y, Yamashina A. Delayed contrast enhancement of MRI in hypertrophic cardiomyopathy. *Magn Reson Imaging*. 2004;22:155–161.

9. Iles L, Pfluger H, Phrommintikul A, Cherayath J, Aksit P, Gupta SN, Kaye DM, Taylor AJ. Evaluation of diffuse myocardial fibrosis in heart failure with cardiac magnetic resonance contrast-enhanced T1 mapping. *J Am Coll Cardiol*. 2008; 52:1574–1580.

10. Flett AS, Hayward MP, Ashworth MT, Hansen MS, Taylor AM, Elliott PM, McGregor C, Moon JC. Equilibrium contrast cardiovascular magnetic resonance for the measurement of diffuse myocardial fibrosis: preliminary validation in humans. *Circulation*. 2010;122:138–144.

11. Sibley CT, Noureldin RA, Gai N, Nacif MS, Liu S, Turkbey EB, Mudd JO, van der Geest RJ, Lima JA, Halushka MK, Bluemke DA. T1 mapping in cardiomyopathy at cardiac MR: comparison with endomyocardial biopsy. *Radiology*. 2012;265: 724–732.

12. Chan W, Duffy SJ, White DA, Gao XM, Du XJ, Ellims AH, Dart AM, Taylor AJ. Acute left ventricular remodeling following myocardial infarction: coupling of regional healing with remote extracellular matrix expansion. *JACC Cardiovasc Imaging*. 2012;5:884–893.

13. Ng AC, Auger D, Delgado V, van Elderen SG, Bertini M, Siebelink HM, van der Geest RJ, Bonetti C, van der Velde ET, de Roos A, Smit JW, Leung DY, Bax JJ, Lamb HJ. Association between diffuse myocardial fibrosis by cardiac magnetic resonance contrast-enhanced T mapping and subclinical myocardial dysfunction in diabetic patients: a pilot study. *Circ Cardiovasc Imaging*. 2012;5:51–59.

14. Ling LH, Kistler PM, Ellims AH, Iles LM, Lee G, Hughes GL, Kalman JM, Kaye DM, Taylor AJ. Diffuse ventricular fibrosis in atrial fibrillation: noninvasive evaluation and relationships with aging and systolic dysfunction. *J Am Coll Cardiol*. 2012;60:2402–2408.

15. Ellims AH, Iles LM, Ling LH, Hare JL, Kaye DM, Taylor AJ. Diffuse myocardial fibrosis in hypertrophic cardiomyopathy can be identified by cardiovascular magnetic resonance, and is associated with left ventricular diastolic dysfunction. *J Cardiovasc Magn Reson*. 2012;14:76.

16. Zeisberg EM, Tarnavski O, Zeisberg M, Dorfman AL, McMullen JR, Gustafsson E, Chandraker A, Yuan X, Pu WT, Roberts AB, Neilson EG, Sayegh MH, Izumo S, Kalluri R. Endothelial-to-mesenchymal transition contributes to cardiac fibrosis. *Nat Med*. 2007;13:952–961.

17. Bucala R, Spiegel LA, Chesney J, Hogan M, Cerami A. Circulating fibrocytes define a new leukocyte subpopulation that mediates tissue repair. *Mol Med*. 1994;1:71–81.

18. Abe R, Donnelly SC, Peng T, Bucala R, Metz CN. Peripheral blood fibrocytes: differentiation pathway and migration to wound sites. *J Immunol*. 2001; 166:7556–7562.

19. Bellini A, Mattoli S. The role of the fibrocyte, a bone marrow-derived mesenchymal progenitor, in reactive and reparative fibroses. *Lab Invest*. 2007;87:858–870.

20. Keeley EC, Mehrad B, Strieter RM. The role of fibrocytes in fibrotic diseases of the lungs and heart. *Fibrogenesis Tissue Repair*. 2011;4:2.

21. Keeley EC, Mehrad B, Strieter RM. The role of circulating mesenchymal progenitor cells (fibrocytes) in the pathogenesis of fibrotic disorders. *Thromb Haemost*. 2009;101:613–618.

22. Kisseleva T, Uchinami H, Feirt N, Quintana-Bustamante O, Segovia JC, Schwabe RF, Brenner DA. Bone marrow-derived fibrocytes participate in pathogenesis of liver fibrosis. *J Hepatol*. 2006;45:429–438.

23. Moeller A, Gilpin SE, Ask K, Cox G, Cook D, Gauldie J, Margetts PJ, Farkas L, Dobranowski J, Boylan C, O'Byrne PM, Strieter RM, Kolb M. Circulating fibrocytes are an indicator of poor prognosis in idiopathic pulmonary fibrosis. *Am J Respir Crit Care Med*. 2009;179:588–594.

24. Sakai N, Wada T, Yokoyama H, Lipp M, Ueha S, Matsushima K, Kaneko S. Secondary lymphoid tissue chemokine (SLC/CCL2)/CCR7 signaling regulates fibrocytes in renal fibrosis. *Proc Natl Acad Sci USA*. 2006;103:14098–14103.

25. Chu PY, Mariani J, Finch S, McMullen JR, Sadoshima J, Marshall T, Kaye DM. Bone marrow-derived cells contribute to fibrosis in the chronically failing heart. *Am J Pathol*. 2010;176:1735–1742.

26. Sopel MJ, Rosin NL, Lee TD, Legare JF. Myocardial fibrosis in response to angiotensin II is preceded by the recruitment of mesenchymal progenitor cells. *Lab Invest*. 2011;91:565–578.

27. Gai N, Turkbey EB, Nazarian S, van der Geest RJ, Liu CY, Lima JA, Bluemke DA. T1 mapping of the gadolinium-enhanced myocardium: adjustment for factors affecting interpatient comparison. *Magn Reson Med*. 2011;65: 1407–1415.

28. Fang L, Moore XL, Chan W, White DA, Chin-Dusting J, Dart AM. Decreased fibrocyte number is associated with atherosclerotic plaque instability in man. *Cardiovasc Res*. 2012;95:124–133.

29. Quan TE, Bucala R. Culture and analysis of circulating fibrocytes. *Methods Mol Med*. 2007;135:423–434.

30. Shao DD, Suresh R, Vakil V, Gomer RH, Pilling D. Pivotal advance: Th-1 cytokines inhibit, and Th-2 cytokines promote fibrocyte differentiation. *J Leukoc Biol*. 2008;83:1323–1333.

31. Phillips RJ, Burdick MD, Hong K, Lutz MA, Murray LA, Xue YY, Belperio JA, Keane MP, Strieter RM. Circulating fibrocytes traffic to the lungs in response to CXCL12 and mediate fibrosis. *J Clin Invest*. 2004;114: 438–446.

32. Mathai SK, Gulati M, Peng X, Russell TR, Shaw AC, Rubinowitz AN, Murray LA, Siner JM, Antin-Ozerkis DE, Montgomery RR, Reilkoff RA, Bucala RJ, Herzog EL. Circulating monocytes from systemic sclerosis patients with interstitial lung disease show an enhanced profibrotic phenotype. *Lab Invest*. 2010;90: 812–823.

33. Wang CH, Huang CD, Lin HC, Lee KY, Lin SM, Liu CY, Huang KH, Ko YS, Chung KF, Kuo HP. Increased circulating fibrocytes in asthma with chronic airflow obstruction. *Am J Respir Crit Care Med*. 2008;178:583–591.

34. Yang L, Scott PG, Giuffre J, Shankowsky HA, Ghahary A, Tredget EE. Peripheral blood fibrocytes from burn patients: identification and quantification of fibrocytes in adherent cells cultured from peripheral blood mononuclear cells. *Lab Invest*. 2002;82:1183–1192.

35. Chesney J, Metz C, Stavitsky AB, Bacher M, Bucala R. Regulated production of type I collagen and inflammatory cytokines by peripheral blood fibrocytes. *J Immunol*. 1998;160:419–425.

36. Mehrad B, Burdick MD, Zisman DA, Keane MP, Belperio JA, Strieter RM. Circulating peripheral blood fibrocytes in human fibrotic interstitial lung disease. *Biochem Biophys Res Commun*. 2007;353:104–108.

37. Pilling D, Vakil V, Gomer RH. Improved serum-free culture conditions for the differentiation of human and murine fibrocytes. *J Immunol Methods*. 2009;351:62–70.